Projection map of the reaction center-light harvesting 1 complex from *Rhodopseudomonas viridis* at 10 Å resolution

Ikuko Ikeda-Yamasaki[a], Takayuki Odahara[b], Kaoru Mitsuoka[c], Yoshinori Fujiyoshi[c], Kazuyoshi Murata[d,*]

[a] *Faculty of Engineering Science, Osaka University, 1-3 Machikaneyama, Toyonaka 560-0043, Japan*
[b] *National Institute of Bioscience and Human Technology, 1-1 Higashi, Tsukuba 305-0046, Japan*
[c] *Department of Biophysics, Faculty of Science, Kyoto University, Kitashirakawa, Sakyo-Ku, Kyoto 606-8224, Japan*
[d] *International Institute for Advanced Research, Matsushita Electric Industrial Co., Ltd., 3-4 Hikaridai, Seika 619-0237, Japan*

Received 14 January 1998

Abstract The photosynthetic reaction center-light harvesting 1 complex from *Rhodopseudomonas viridis* was purified and reconstituted into two-dimensional crystals. The single-layered crystalline sheets with lattice parameters $a = b = 133.3$ Å and $\gamma = 120°$ were investigated by electron cryo-microscopy and the projection map at 10 Å resolution was calculated. The opening diameter of the light-harvesting ring of 72 Å is sufficient to allow slight movement of the reaction center within the ring. Based on characteristic features observed in the projection map, the mechanism of energy transfer from the light-harvesting 1 complex to the reaction center was discussed.

Key words: Electron cryo-microscopy; Two-dimensional crystal; Reaction center-light harvesting 1 complex; *Rhodopseudomonas viridis*

1. Introduction

Photosynthesis is one of the most fundamental biological reactions. The first step of the photosynthetic reaction in purple non-sulfur and sulfur bacteria is the absorption of a photon by a light-harvesting antenna protein-pigment (LH) complex. Subsequently, the absorption energy is transferred to the bacteriochlorophyll (BChl) special pair of the reaction center (RC). The electron transfer within the RC and the energy transduction across the membrane are understood in great detail by the atomic structures of the RCs from *Rhodopseudomonas* (*Rp.*) *viridis* [1] and *Rhodobacter* (*Rb.*) *sphaeroides* [2], as well as by active biophysical and photochemical studies. However, there are still open questions concerning the initial energy transfer from the LH1 complex to the RC. Therefore, it is hoped that a detailed structure of the complex which the RC forms with LH1 will bring insight into the mechanism of excitation energy transfer from the LH1 complex to the RC.

Several RC-LH1 complexes from various photosynthetic bacteria have already been studied by electron microscopy, revealing that the RC is surrounded by a ring composed of LH1 subunits [3–6]. Structural data, in combination with biochemical and biophysical studies, have led to the generally accepted process that a photon absorbed by LH1 excites an electron and that the excitation energy is passed on to the BChl special pair in the RC [7]. Unfortunately, the structures of RC-LH1 complexes have only been determined to a rather moderate resolution so far. This is due to the limited crystallinity of the two-dimensional (2D) arrays which were studied and also due to the negative stain which was used to contrast the specimens. Therefore, these studies did not allow elucidation of the detailed relationship between the structure and the function of the RC-LH1 complex.

We chose *Rp. viridis* as a very promising model system to elucidate the structure of the RC-LH1 complex for several reasons, as follows. *Rp. viridis* has a relatively simple photosynthetic system because only a single type of LH complex is expressed. The RC-LH1 complex constitutes more than 90% of the total protein in the thylakoid membranes and thus it is easy to purify large quantities of the RC-LH1 complex. Moreover, the structure of the RC has already been solved at atomic resolution [1] and the photosynthetic reaction has been extensively studied by biochemical and biophysical techniques. Finally, the RC-LH1 complex from *Rp. viridis* already forms 2D crystalline arrays in the photosynthetic membranes indicating an intrinsic propensity of this complex to form 2D crystals. Thus, the RC-LH1 complex from *Rp. viridis* is highly amenable to structural studies which will help us to understand the initial photosynthetic reaction steps.

To overcome the resolution limitations encountered by previous investigators due to the lack of crystallinity of the 2D arrays found in photosynthetic membranes of *Rp. viridis*, we purified the RC-LH1 complexes and reconstituted them into 2D crystals in the presence of phospholipids. The resulting 2D crystals were studied by electron cryo-microscopy to avoid resolution limitations imposed by negative staining. Recently remarkable progress in electron cryo-microscopy has even allowed the determination of the near-atomic structure of 2D crystallized proteins [8,9]. High resolution electron microscopy of 2D crystals is also especially well suited for integral membrane proteins, because it allows visualization of the interactions between integral membrane proteins and the surrounding lipid bilayer. Here, we present the successful reconstitution of detergent-solubilized RC-LH1 complexes from *Rp. viridis* into well-ordered 2D crystals and the projection map at 10 Å resolution.

2. Materials and methods

2.1. Purification and two-dimensional crystallization of RC-LH1 complexes

For 2D crystallization, photosynthetic membranes isolated from *Rp. viridis* were solubilized with 1% (w/v) 3-[(3-cholamidopropyl) dimethylammonio]-1-propanesulfonate (CHAPS; Dojin) and the RC-LH1 complexes were purified by polyacrylamide gel electrophoresis [10]. Subsequently, the RC-LH1 complexes were applied to a CL-4B

*Corresponding author. Fax: (81) (774) 98-2575.
E-mail: murata00@crl.mei.co.jp

PII S0014-5793(98)00300-7

gel filtration column (Pharmacia). The purified RC-LH1 complexes were mixed with detergent-solubilized soybean PC to give a final protein concentration of 1 mg/ml and a lipid-to-protein ratio of 1. The mixture was dialyzed against detergent-free sample buffer (10 mM Tris-HCl, pH 8.0, 1 mM EDTA, 5% glycerol and 0.05% NaN_3) at 25–30°C for 4–7 days, using L-shaped glass capillary tubes and dialysis membranes with a 50 kDa cut-off (SpectraPor 7, Spectrum). To check the outcome of dialysis experiments for 2D crystallization, samples were negatively stained with 2% (w/v) uranyl acetate and observed with a JEM1010 electron microscope (JEOL) at a nominal magnification of 20 000× and operated at an acceleration voltage of 100 kV.

2.2. Electron cryo-microscopy and image processing

RC-LH1 2D crystals were prepared for high resolution electron microscopy by adding trehalose to a final concentration of 3% [11]. The sample was adsorbed to a carbon-coated molybdenum grid and rapidly frozen in liquid ethane. Electron micrographs were taken with a JEM-3000SFF electron microscope, operated at an acceleration voltage of 300 kV and equipped with a field emission gun and a liquid helium stage [12]. For data collection, the specimen was kept at 4.2 K and imaged at a nominal magnification of 40 000× using an electron dose of 10 $e^-/Å^2$. Micrographs, recorded on Kodak SO163 film, were developed for 14 min in Kodak D-19 developer. Well-ordered crystalline areas were selected by optical diffraction and areas of 8000×6000 pixels were digitized with a LeafScan45 line-illuminating micro-densitometer [13] using a step size of 5 μm, corresponding to 1.5 Å on the specimen. Bacteriorhodopsin 2D crystals were used as a reference for precise determination of the lattice parameters of the RC-LH1 2D crystals. The MRC image processing programs [14] were used for lattice unbending, CTF correction and merging of the images as described in [15].

3. Results and discussions

3.1. Two-dimensional crystallization of the RC-LH1 complexes from Rp. viridis

For 2D crystallization, the choice of detergent for purification and subsequent reconstitution is of primary importance for the protein stability and the outcome of 2D crystallization trials [16]. We used CHAPS for solubilization, purification and 2D crystallization steps because of its mildness and high critical micelle concentration. The RC-LH1 complex was stable in CHAPS and no change in the absorption spectrum of the complex was observed upon solubilization.

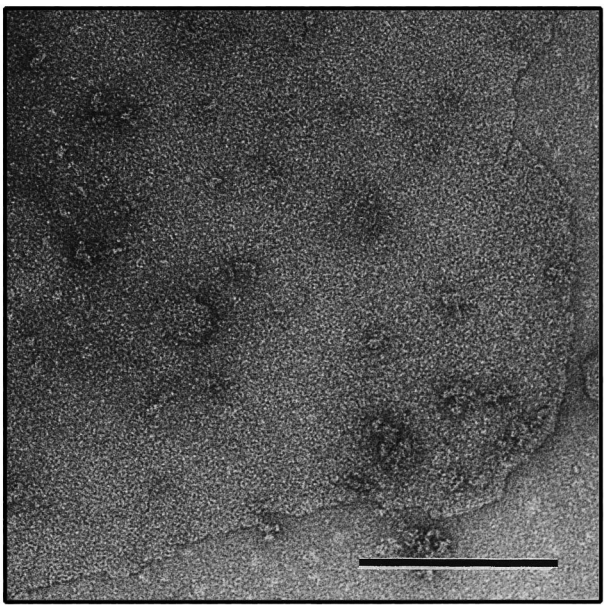

Fig. 1. An electron micrograph of a negatively stained RC-LH1 2D crystal (scale bar indicates 200 nm).

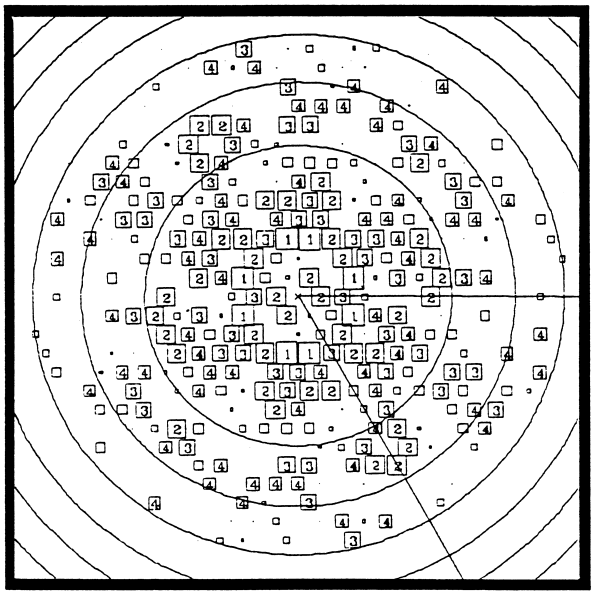

Fig. 2. Calculated diffraction pattern of the best image from a trehalose-embedded RC-LH1 2D crystal. The Fourier components were measured to 10 Å resolution and the numbers and size of the boxes indicate the IQ values of the reflections as defined in [26]. The concentric ellipses represent zero transitions of the contrast transfer function (CTF) and the reciprocal lattice vectors are also depicted.

Beside detergents, lipids used for reconstitution and the lipid-to-protein ratio (LPR) are also known to be critical for the success of crystallization. The lipids we tested included dimyristoyl PC (DMPC), which was used for 2D crystallization of LH2 from *Rhodovulum sulfidophilum* [17], and dioleoyl PC (DOPC), which was used previously for reconstitution of LH1 [18] as well as the RC-LH1 complex from *Rb. rubrum* [6]. Moreover, we tried lipid mixtures such as egg yolk PC which yielded highly ordered crystals of Ca^{2+}-ATPase [19] and soybean PC suitable for 2D crystallization of cytochrome reductase [20]. In our case, synthesized PCs (DMPC, DOPC) and egg yolk PC did not produce well-ordered 2D crystals of the RC-LH1 complex from *Rp. viridis*. On the other hand, stable and highly ordered 2D crystals formed upon reconstitution with soybean PC. The LPR also influenced the quality of the RC-LH1 2D crystals. The optimum LPR (w/w) for the crystallization was found to be 1. At lower LPRs, the complexes aggregated while higher LPRs led to reduced crystallinity of the reconstituted 2D arrays.

When reconstitution experiments were successful, membranes with a diameter of 1–3 μm formed after 1–2 days. A micrograph of a negatively stained RC-LH1 2D crystal is shown in Fig. 1. All crystals showed the same hexagonal lattice with lattice parameters $a = b = 133.3$ Å and $\gamma = 120°$. These values are similar to the lattice parameters of the 2D crystalline patches occurring in the native photosynthetic membrane [3,4]. Moreover, the absorption spectra of native photosynthetic membranes and reconstituted 2D crystals were identical (data not shown), which suggests that our 2D crystals represent the native structure and arrangement of the RC-LH1 complex from *Rp. viridis*.

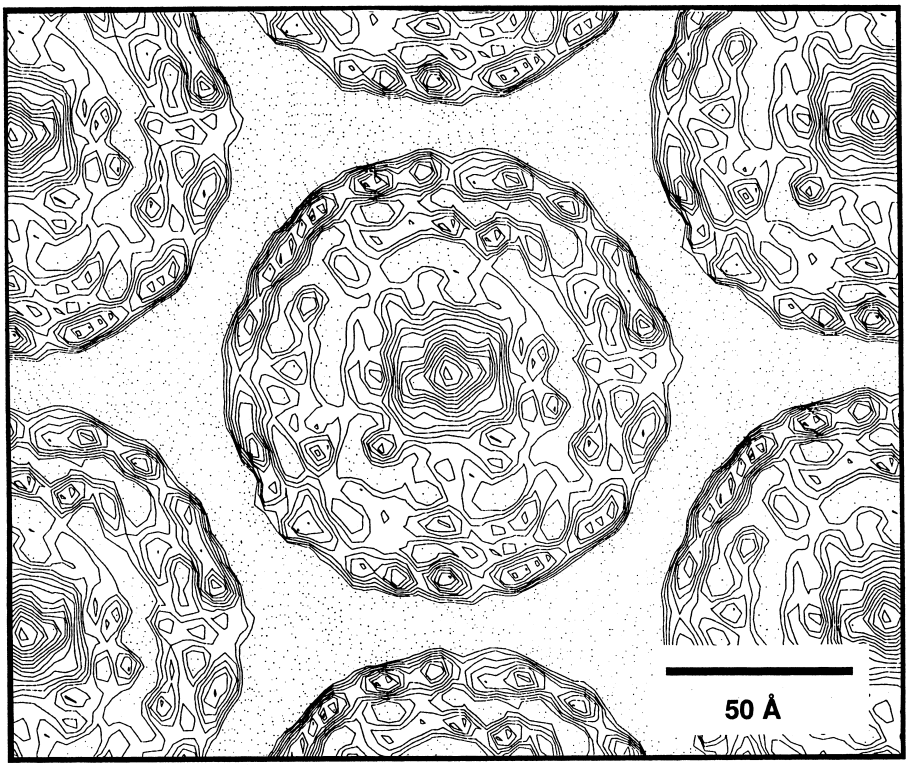

Fig. 3. Unsymmetrized projection map of the RC-LH1 complex from *Rp. viridis* calculated to 10 Å resolution using the Fourier components from eight images. The phases and amplitudes used for this map were only corrected for the phase-contrast transfer function. Contours are calculated arbitrarily and the solid lines indicate density above the mean value. The scale bar indicates 50 Å.

3.2. Image analysis

To illustrate the quality of our RC-LH1 2D crystals, the computer-generated diffraction pattern of the best image is shown in Fig. 2. The statistics of the eight images which were merged to calculate the final projection map are given in Table 1. The overall phase residual of the final data set up to 10 Å resolution determined by comparison of 954 independent phase measurements is 32.4° (phase residuals in resolution shells are given in Table 1).

3.3. Structure of the RC-LH1 complexes and its implication for the mechanism of energy transfer from LH1 to RC

Our projection map of the RC-LH1 complex from *Rp. viridis* at a resolution of 10 Å reveals three clearly distinguishable regions of density, an asymmetric central core and two concentric rings surrounding it (Fig. 3). In accordance with previous work, we interpret the core density as a RC molecule and the two concentric rings as a LH1 complex [3,4]. The average diameters of the inner and the outer rings of the LH1 complex are 80 Å and 110 Å, respectively. These diameters are slightly bigger than those determined for the LH1 complex from *Rs. rubrum* [18]. Interestingly, the density of the outer ring of the LH1 complex in our projection map appears to be significantly higher than that of the inner ring. LH1 from *Rp. viridis* consists of three polypeptides (α, β and γ) which are expressed at a stoichiometric ratio of 1:1:1 [23] and each polypeptide contributed to one transmembrane α-helix of the LH complexes. Therefore, every LH1 subunit

Table 1
Electron crystallographic image data

2D crystals		
Unit cell dimension	$a = b = 133.3 \pm 1.3$ Å $\gamma = 120°$	
Crystallographic space group	p1	
Phase determination by image processing		
Resolution (Å)	10	
Range of underfocus (Å)	13 100–22 000	
Total no. of observed reflections	954	
Resolution range (Å)	Averaged reflections[a]	Phase residual
150.0–30.0	191	13.6
30.0–20.0	160	26.3
20.0–15.0	191	28.1
15.0–12.0	200	36.8
12.0–10.0	212	53.3
Total: 150.0–10.0	954	32.4

[a]Averaged when two or more reflections of IQ ≤ 7 were observed.

from this organism is expected to contain three transmembrane α-helices. From the higher density for the outer ring in our projection map, we interpreted that the outer ring would consist of two membrane-spanning helices per subunit. The inner ring with the lower density would accordingly comprise the third membrane-spanning helix of the subunit.

This feature distinguishes the structure of LH1 from those of the two bacterial LH2 complexes studied so far, the LH2s from *Rp. acidophila* and *Rs. molischianum* determined by X-ray diffraction analysis [21,22]. These two LH2 complexes consist of two types of polypeptides (α and β) and a single subunit of the complexes has two transmembrane helices. The transmembrane helices of the α-polypeptides, which run perpendicular to the membrane plane, are shown to be closely packed and arranged on an inner circle, while the α-helices of the β-polypeptides, which are tilted with respect to the membrane normal, are placed in a wide row on an outer circle and hold BChl molecules between them. Therefore, the density of the inner ring of the LH2 complex is shown to be higher than that of the outer ring unlike that of *Rp. viridis* LH1. This difference could reflect the different radial position of the BChl molecules in LH1 and LH2 complexes, and therefore help to transfer energy efficiently from the BChl molecules in the opposite directions in LH1 and LH2 complexes, towards the inside of the ring and towards the outside, respectively.

The number of LH1 subunits forming the ring around the RC is another point of interest in this study field. Karrasch et al. reported that the LH1 complex from *Rs. rubrum* is formed from 16 subunits and each subunit consists of two transmembrane α-helices according to the 8.5 Å projection map provided by cryo-electron microscopy and digital image processing [18]. From negative stain studies of *Rp. viridis* RC-LH1 complex in thylakoid membranes, it was reported that the central core is surrounded by a ring of 12 and six subunits on the cytoplasmic and the exoplasmic side, respectively [4]. However, our 10 Å projection map of the LH1 subunits could not give conclusive evidence of the number of subunits, even though we tried to calculate the rotational power spectrum using RFILTIM [24]. Furthermore, our map could not exclude the possibility of non-periodic arrangement of the subunits in the LH1 ring.

The light energy absorbed in the BChl molecules in the LH1 complex is transferred to the BChl special pair of the RC. Therefore, the distance between these two kinds of BChl molecules is one of the important parameters to understand the excitation energy transfer in the primary reaction of photosynthesis. α- and β-polypeptides of *Rp. viridis* LH1 contain one (α36) and two histidine (β19 and β37) residues, respectively and the positions of the two histidine residues (α36 and β37) are similar to those in the α- and β-polypeptides of *Rp. acidophila* LH2 [21]. Therefore, the BChl molecules in *Rp. viridis* LH1 are also expected to be supported by the histidine residues on the α- and β-polypeptides in the same manner. Assuming these BChl molecules are sandwiched between the two transmembrane helices, the distance from the center of the complex to the expected position of the BChl molecules in the LH1 ring is 43–55 Å in the projection map. If the special pair is located in the center of the complex, the light energy absorbed in LH1 should be transferred at this distance. However, the opening diameter of the LH1 ring of 72 Å is slightly larger than the major axis of the RC. Therefore, the RC may move within the LH1 ring, and if we assume an eccentric position of the RC within the LH1 ring, the distance between the special pair and the position of the BChls within the LH1 ring can decrease to about 37–49 Å. However, the trapping time of the excitation energy in the LH1 complex measured for the RC-LH1 complex from *Rp. viridis* containing photochemically active and inactive RC suggests a distance of 17 Å between the special pair of the RC and the BChl molecules in LH1 ring [25]. We could not explain this distance from our projection map. A more minute explanation for the transfer of excitation energy from the LH1 complex to the RC has to await the determination of a three-dimensional structure at near-atomic resolution.

Acknowledgements: We thank M. Hara for fruitful discussions, Y. Fujita and Y. Cheng for critical reading, K. Iwasaki, T. Hirai, and K. Yonekura for computational support and J. Hasegawa for calibration of the crystal lattice.

References

[1] Deisenhofer, J., Epp, O., Miki, K., Huber, R. and Michel, H. (1985) Nature 318, 618–623.
[2] Allen, J.P., Feher, G., Yeates, T.O., Komiya, H. and Rees, D.C. (1987) Proc. Natl. Acad. Sci. USA 84, 5730–5734.
[3] Miller, K.R. (1982) Nature 300, 53–55.
[4] Stark, W., Kühlbrandt, W., Wildhaber, I., Wehrli, E. and Muhlethaler, K. (1984) EMBO J. 3, 777–783.
[5] Engelhardt, H., Engel, A. and Baumeister, W. (1986) Proc. Natl. Acad. Sci. USA 83, 8972–8976.
[6] Walz, T. and Ghosh, R. (1997) J. Mol. Biol. 265, 107–111.
[7] Van Grondelle, R., Dekker, J.P., Gillbro, T. and Sundstrom, V. (1994) Biochim. Biophys. Acta 1187, 1–65.
[8] Henderson, R., Baldwin, J.M., Ceska, T.A., Zemlin, F., Beckmann, E. and Downing, K.H. (1990) J. Mol. Biol. 213, 899–929.
[9] Kühlbrandt, W., Wang, D.N. and Fujiyoshi, Y. (1994) Nature 367, 614–621.
[10] Hara, M., Namba, K., Hirata, Y., Majima, T., Kawamura, S., Asada, Y. and Miyake, J. (1990) Plant Cell Physiol. 31, 951–960.
[11] Kimura, Y., Vassylyev, D.G., Miyazawa, A., Kidera, A., Matsushima, M., Mitsuoka, K., Murata, K., Hirai, T. and Fujiyoshi, Y. (1997) Nature 389, 206–211.
[12] Fujiyoshi, Y., Mizusaki, T., Morikawa, K., Yamagishi, H., Aoki, Y., Kihara, H. and Harada, Y. (1991) Ultramicroscopy 38, 241–251.
[13] Mitsuoka, K., Murata, K., Kimura, Y., Namba, K. and Fujiyoshi, Y. (1997) Ultramicroscopy 68, 109–121.
[14] Crowther, R.A., Henderson, R. and Smith, J.M. (1996) J. Struct. Biol. 116, 9–16.
[15] Amos, L.A., Henderson, R. and Unwin, N. (1982) Prog. Biophys. Mol. Biol. 39, 183–231.
[16] Kühlbrandt, W. (1992) Q. Rev. Biophys. 25, 1–49.
[17] Montoya, G., Cyrklaff, M. and Sinning, I. (1995) J. Mol. Biol. 250, 1–10.
[18] Karrasch, S., Bullough, P.A. and Ghosh, R. (1995) EMBO J. 14, 631–638.
[19] Stokes, D.L. and Green, N.M. (1990) Biophys. J. 57, 1–14.
[20] Hovmöller, S., Slaughter, M., Berriman, J., Karlsson, B., Weiss, H. and Leonard, K. (1983) J. Mol. Biol. 165, 401–406.
[21] McDermott, G., Prince, S.M., Freer, A.A., Hawthornthwaite-Lawless, A.M., Papiz, M.Z., Cogdell, R.J. and Isaacs, N.W. (1995) Nature 374, 517–521.
[22] Koepke, J., Hu, X., Muenke, C., Schulten, K. and Michel, H. (1996) Structure 4, 581–597.
[23] Brunisholz, R.A., Jay, F., Suter, F. and Zuber, H. (1985) Biol. Chem. Hoppe-Seyler 366, 87–98.
[24] Crowther, R.A. and Amos, L.A. (1971) J. Mol. Biol. 60, 123–130.
[25] Zhang, F.G., Gillbro, T., Van Grondelle, R. and Sundstrom, V. (1992) Biophys. J. 61, 694–703.
[26] Henderson, R., Baldwin, J.M., Downing, K., Lepault, J. and Zemlin, F. (1986) Ultramicroscopy 19, 147–178.